Nonlinear Dynamics manuscript No.
(will be inserted by the editor)

A complementarity approach for the computation of periodic oscillations in piecewise linear systems

Valentina Sessa · Luigi Iannelli · Francesco Vasca · Vincent Acary

Received: date / Accepted: date

Abstract Piecewise linear (PWL) systems can exhibit quite complex behaviors. In this paper, the complementarity framework is used for computing periodic steady-state trajectories of systems which consist of linear time-invariant systems with PWL, possibly set-valued, feedback relations. The computation of the periodic solutions is formulated in terms of mixed quadratic complementarity problems. The proposed procedure is generalized also for the case of unknown period and phase of the steady-state oscillations by including suitable anchor equations as further problem constraints. The complementarity problem solution is shown to provide an accurate prediction of the steady-state (stable and unstable) oscillation and corresponding period. This is demonstrated through numerical investigations of several PWL systems of practical interest: a neural oscillator, a deadzone feedback system, a stick-slip system and a repressilator.

Keywords Piecewise linear systems · Complementarity systems · Periodic solutions · Autonomous systems

V. Sessa
Instituto de Matemática Pura e Aplicada (IMPA), Estrada Dona Castorina 110, Rio de Janeiro, RJ, Brazil.
E-mail: valsessa@impa.br

L. Iannelli · F. Vasca
Department of Engineering, University of Sannio, Piazza Roma 21, 82100 Benevento, Italy.
E-mail: luigi.iannelli,vasca@unisannio.it

V. Acary
INRIA, Bipop team-project, Inovallee de Montbonnot, 655 avenue, Europe 38334 Saint Ismier cedex, France.
E-mail: vincent.acary@inria.fr

© 2016 by Springer-Verlag Berlin Heidelberg and Mathematical Optimization Society.
This is the accepted version of the paper.
The final publication is available at link.springer.com. DOI: 10.1007/s11071-016-2758-5

1 Introduction

Piecewise linear (PWL) models can represent a wide class of practical systems and can exhibit interesting nonlinear behaviors such as periodic steady-state oscillations. In this paper, we consider the problem of the computation of periodic solutions for linear time-invariant dynamical systems whose inputs are related to the outputs through a static multi input–multi output PWL relation, possibly set-valued. That class of dynamical systems has attracted a considerable interest in the literature, because such representation is sufficiently easy to deal with and, at the same time, it allows to capture even complex behaviours arising in many practical systems. We can mention electrical circuits where the current–voltage characteristics of some devices can be considered as piecewise linear, such as nonlinear resistors [1], ideal diodes and switches [2,3], or mechanical systems with Coulomb friction [4]. In those applications, the steady-state behaviour is generally depicted by a periodic motion [5,6]. Since they tend to periodically oscillate also when no external excitation is applied, the period related to the periodic solution is difficult to be predicted a priori. In the literature, various mathematical methods, basically classified as time-domain or frequency-domain, have been proposed to compute the steady-state periodic solution and its period. Time-domain approaches are based mainly on the so-called shooting method which determines the periodic solution by solving a sequence of nonlinear initial value problems through the Newton-Raphson method [7–9]. The main drawback of this method is the evaluation of the sensitivity matrix, which is often computationally expensive and becomes even more complicated for nonsmooth systems [10–12] where often the discontinuity is approximated by a smooth function [13,14]. In frequency-domain, harmonic balance is the classical technique used for determining the steady-state behaviour of nonlinear autonomous systems that exhibit a single periodic attractor [15]. The describing function method (i.e., harmonic balance with a single harmonic) provides simpler results about the existence of a periodic oscillation and its parameters (the amplitude and the period) [16, 17], but it is not able to accurately predict them, particularly when the system under consideration does not satisfy the assumption of filtering out the higher-order harmonics [18]. In [19], an extension of the harmonic balance method for computing the rotary and oscillatory periodic motion of a nonlinear smooth system is proposed. Mixed time-frequency-domain approaches are presented in [20] and [21]. In the first paper, a nonlinear oscillator is analysed by linearizing the system along the solution predicted by the harmonic balance technique and then by computing the Floquet's multipliers by using a time-domain numerical algorithm. Instead, in [21], the harmonic balance method is implemented together with the envelope following method in time domain. Such approach is used to compute the steady-state behaviour and the associated period of nonlinear circuits forced by two input signals with different oscillation frequencies.

The recent literature has shown the complementarity framework being useful for investigating PWL systems [22–24] and a particular class of hybrid sys-

tem [25,26]. In [27,28] and [29] it has been shown how the linear (or mixed linear) complementarity representation of the feedback characteristic allows to represent the discretized closed-loop system as a linear complementarity system. Including the periodicity constraint into a corresponding linear complementarity problem represents a method for computing periodic solutions in autonomous Lur'e systems. The main drawback of the previous approaches is that the period must be known a priori or, at least, a certain estimation of the period must be obtained by using, for instance, the describing function technique.

Instead, in [30], the period is considered as a further unknown and it is computed together with the periodic solution by constructing a suitable mixed complementarity problem. The scope of this paper is to extend previous authors results by proposing techniques based on complementarity problems for computing the periodic solution in PWL systems.

The paper is organized as follows. In Section 2, we present the autonomous PWL systems considered in this paper and we give some preliminaries about the complementarity problems and the complementarity model of a class of PWL characteristics. Section 3 shows how to formulate a mixed quadratic complementarity problem (MQCP) for computing a periodic solution together with the period. In Section 4, two specific cases are analyzed: when the PWL system has also equilibrium points and when the period of the oscillation is known. In Section 5, we show the effectiveness of the proposed approach by considering different steady-state behaviours in several PWL systems of practical interest. In particular, we consider a stable periodic solution in a neural oscillator, an unstable periodic solution in a deadzone feedback system, a sliding periodic solution in a stick-slip system and the periodic oscillation belonging to a repressilator. The paper is concluded in Section 6.

2 Preliminaries

Let us introduce first some notation and preliminary definitions. Let the $\mathrm{col}(\cdot)$ operator indicate a vector obtained by stacking in a unique column the column vectors in its argument, $\mathbb{R}^N_+$ is the set of nonnegative N-dimensional real vectors, I_N denotes the $N \times N$ identity matrix and 1_N, ∞_N are the N-dimensional vectors whose components are ones and infinity, respectively. The symbol $\otimes$ indicates the Kronecker product. The following block circulant matrix notation is adopted

$$\Gamma_N(\mathcal{B}_1, \mathcal{B}_2) = \begin{bmatrix} \mathcal{B}_1 & 0 & \cdots & \cdots & 0 & \mathcal{B}_2 \\ \mathcal{B}_2 & \mathcal{B}_1 & 0 & \cdots & \cdots & 0 \\ 0 & \mathcal{B}_2 & \mathcal{B}_1 & 0 & \cdots & \vdots \\ \vdots & \ddots & \ddots & \ddots & \ddots & \\ 0 & \cdots & 0 & \mathcal{B}_2 & \mathcal{B}_1 & 0 \\ 0 & 0 & \cdots & 0 & \mathcal{B}_2 & \mathcal{B}_1 \end{bmatrix}, \tag{1}$$

where $\mathcal{B}_1$ and $\mathcal{B}_2$ are square matrices of the same dimension and N is the number of times that $\mathcal{B}_1$ is repeated on the main diagonal.

The mixed quadratic complementarity problem (MQCP) is another important ingredient of this paper. It is defined as follows. Given a function $\varphi(z) : \mathbb{R}^r \to \mathbb{R}^r$, a square matrix $M \in \mathbb{R}^{r\times r}$, a vector $q \in \mathbb{R}^r$, and lower and upper bounds $\ell, u \in \mathbb{R}^r \cup \{-\infty, +\infty\}^r$, a MQCP is to

$$\begin{aligned} \text{find} \quad & z \in \mathbb{R}^r,\ w \in \mathbb{R}^r_+,\ v \in \mathbb{R}^r_+ && \text{(2a)}\\ \text{s.t.} \quad & \varphi(z) + Mz + q = w - v && \text{(2b)}\\ & \ell \leqslant z \leqslant u,\ (z-\ell)^\top w = 0,\ (u-z)^\top v = 0, && \text{(2c)} \end{aligned}$$

where $\varphi(z)$ is a vector of quadratic forms in z and the inequalities are meant componentwise. If ℓ and u are finite, the continuity of $F(z) = \varphi(z) + Mz + q$ ensures the existence of solutions. More results about the existence of solutions for complementarity problems and variational inequality (VI) can be found in [31]. Recall that every (nonlinear) complementarity problem as in (2) is a variational inequality (VI). When the term $\varphi(z)$ does not appear in (2a), the MQCP becomes a mixed *linear* complementarity problem (MLCP) [32]. Moreover, if the upper bound u has all infinity components and $\ell = 0$, one gets $v = 0$ and the problem reduces to the classical linear complementarity problem with w and z being the usual complementarity variables [33].

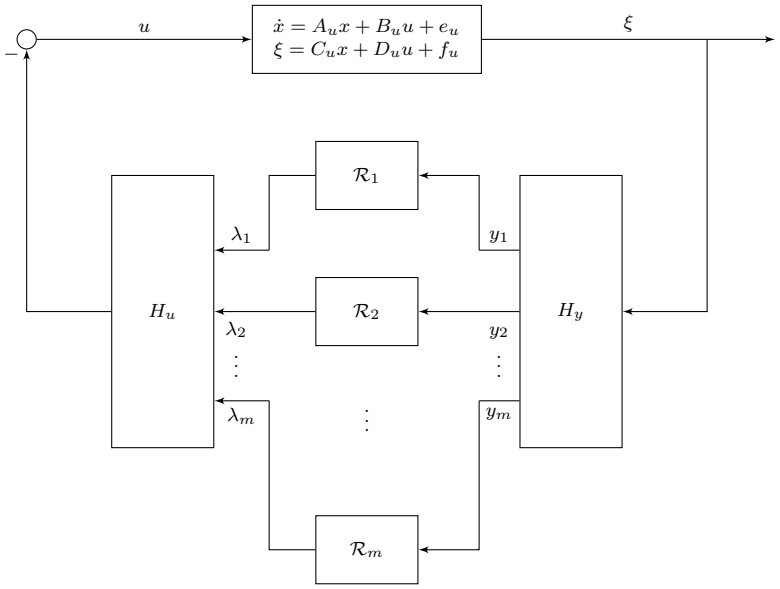

Fig. 1 Block diagram of a PWL system.

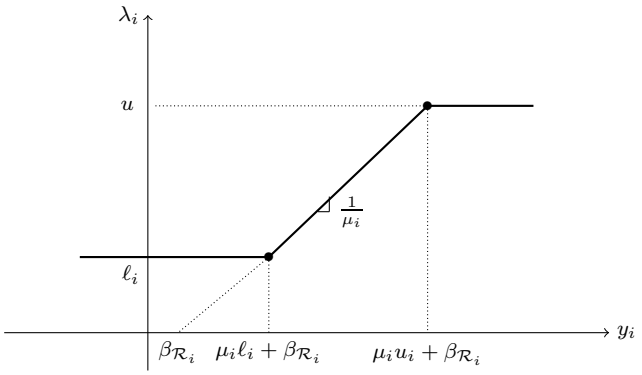

Fig. 2 PWL saturation-like characteristic with $\mu_i > 0$.

The class of systems of interest can be represented by the block scheme in Fig. 1, where the dynamical system is described by

$$\dot{x} = A_u x + B_u u + e_u \tag{3a}$$
$$\xi = C_u x + D_u u + f_u \tag{3b}$$
$$u = -H_u \lambda \tag{3c}$$
$$y = H_y \xi, \tag{3d}$$

with $A_u \in \mathbb{R}^{n\times n}$, $B_u \in \mathbb{R}^{n\times p}$, $C_u \in \mathbb{R}^{p\times n}$, $D_u \in \mathbb{R}^{p\times p}$, $e_u \in R^n$, $f_u \in \mathbb{R}^p$, $y = \mathrm{col}(y_1, y_2, \ldots, y_m)$, $\lambda = \mathrm{col}(\lambda_1, \lambda_2, \ldots, \lambda_m)$, $H_y \in \mathbb{R}^{m\times p}$ and $H_u \in \mathbb{R}^{p\times m}$. Each block $\mathcal{R}_i$ consists of a scalar saturation-like characteristic as in Fig. 2. Such characteristic with finite $\beta_{\mathcal{R}_i}$, $\ell_i, u_i \in \mathbb{R}$, $\ell_i < u_i$ and $\mu_i \geqslant 0$ can be represented in the following mixed linear complementarity form

$$\mu_i\lambda_i - y_i + \beta_{\mathcal{R}_i} = w - v \tag{4a}$$
$$\ell_i \leqslant \lambda_i \leqslant u_i,\ (\lambda_i - \ell_i)w = 0,\ (u_i - \lambda_i)v = 0, \tag{4b}$$

with $w \geqslant 0$ and $v \geqslant 0$. If $\mu_i > 0$, for any given $y_i \in \mathbb{R}$ the MLCP (4) has a unique solution λ_i [34]. Therefore, in order to show that the MLCP (4) corresponds to the relation in Fig. 2, it is enough to verify that the feasible values of λ_i correspond to values of y_i belonging to the saturation characteristic. In particular, if $\lambda_i = \ell_i$ from (4b) it follows $v = 0$ and, since $w \geqslant 0$, one obtains $y_i \leqslant \mu_i\ell_i + \beta_{\mathcal{R}_i}$, that corresponds to the lower constant saturated piece of the characteristic. If $\ell_i < \lambda_i < u_i$ from the second and third constraints in (4b) it follows $w = v = 0$ and from (4a) one obtains $y_i = \mu_i\lambda_i + \beta_{\mathcal{R}_i}$, that corresponds to the linear interval of the saturation characteristic. Finally if $\lambda_i = u_i$, one obtains $w = 0$ and $y_i \geqslant \mu_i u_i + \beta_{\mathcal{R}_i}$, which corresponds to the upper saturation of the characteristic. If $\mu_i = 0$ the model (4) represents set-valued characteristics. Indeed it is easy to verify that for $\mu_i = 0$ the model (4) represents a set-valued step function.

By collecting (4) and by defining $\mathcal{R} = \mathrm{col}(\mathcal{R}_1, \mathcal{R}_2, \ldots, \mathcal{R}_m)$, one can write the relation between y and λ as follows

$$\begin{aligned} \text{find} \quad & \lambda \in \mathbb{R}^m,\ w \in \mathbb{R}^m_+,\ v \in \mathbb{R}^m_+ && \text{(5a)} \\ \text{s.t.} \quad & M_{\mathcal{R}}\lambda - y + \beta_{\mathcal{R}} = w - v && \text{(5b)} \\ & \ell_{\mathcal{R}} \leqslant \lambda \leqslant u_{\mathcal{R}},\ (\lambda - \ell_{\mathcal{R}})^\top w = 0,\ (u_{\mathcal{R}} - \lambda)^\top v = 0, && \text{(5c)} \end{aligned}$$

with $M_{\mathcal{R}} = \mathrm{diag}\{\mu_1, \mu_2, \ldots, \mu_r\} \in \mathbb{R}^{m\times m}$, $\ell_{\mathcal{R}} = \mathrm{col}(\ell_1, \ell_2, \ldots, \ell_m) \in \mathbb{R}^m$, $u = \mathrm{col}(u_1, u_2, \ldots, u_m) \in \mathbb{R}^m$ and $\beta_{\mathcal{R}} = \mathrm{col}(\beta_{\mathcal{R}_1}, \beta_{\mathcal{R}_2}, \ldots, \beta_{\mathcal{R}_m}) \in \mathbb{R}^m$.

The model (5) includes the representation of many typical PWL functions such as mininum, maximum, relay, deadzone and PWL characteristics obtained by linear combinations of these ones.

We now obtain a compact representation for the closed-loop system in Fig. 2. By substituting (3c) in (3a) and (3b), and (3b) in (3d) and by taking

$$\begin{aligned} A &= A_u && \text{(6a)} \\ B &= B_u H_u && \text{(6b)} \\ C &= H_y C_u && \text{(6c)} \\ D &= H_y D_u H_u && \text{(6d)} \\ e &= e_u && \text{(6e)} \\ f &= H_y f_u, && \text{(6f)} \end{aligned}$$

we obtain the following dynamical system

$$\begin{aligned} \dot{x} &= Ax + B(-\lambda) + e && \text{(7a)} \\ y &= Cx + D(-\lambda) + f && \text{(7b)} \\ (y, \lambda) &\in \mathcal{R}, && \text{(7c)} \end{aligned}$$

with $\mathcal{R} = \mathrm{col}(\mathcal{R}_1, \mathcal{R}_2, \ldots, \mathcal{R}_m)$ given by (5) and $(y_i, \lambda_i) \in \mathcal{R}_i$, $i = 1, \ldots, m$.

The class of systems (7) is the one considered in this paper where (A, B, C) is a minimal state space realization with $A \in \mathbb{R}^{n\times n}$, $B \in \mathbb{R}^{n\times m}$, $C \in \mathbb{R}^{m\times n}$, $D \in \mathbb{R}^{m\times m}$, $e \in \mathbb{R}^n$ and $f \in \mathbb{R}^m$ all being constant and the time derivative is meant almost everywhere. It is assumed that for every initial condition $x(t_0)$ the system (7) has an absolutely continuous solution $x(t) : [t_0, +\infty) \mapsto \mathbb{R}^n$ that satisfies (7) for almost every $t \geqslant t_0$. A solution $x(t)$ of the system (7) is *periodic* if there exists a positive real number T such that $x(t + T) = x(t)$ for any $t \geqslant 0$. The stability concepts and definitions typically used for systems and equilibria can be also applied to periodic solutions which can be stable, asymptotically stable and unstable [35].

In the next section, it is shown how the combination of (5) with the discretized version of (7a)–(7b) allows to construct a MQCP for the computation of periodic solutions of (7).

3 Computation of periodic oscillations

Let $x(t)$ be a nonconstant periodic solution of (7) with unknown period, say T. The dynamical model (7) can be normalized with respect to the unknown period by using the time scaling $t = T\tau$, where τ is a dimensionless time variable. Then (7) can be rewritten as

$$x' = TAx + TB(-\lambda) + Te \tag{8a}$$
$$y = Cx + D(-\lambda) + f \tag{8b}$$
$$(y, \lambda) \in \mathcal{R}, \tag{8c}$$

where x' is the derivative with respect to τ. Any periodic solution of (7) with period T will correspond to a periodic solution of (8) with period 1. Note that the right hand side of (8a) is quadratic with respect to the unknowns T, x and λ.

By using (5) and (8), the problem of computing the periodic solution is to

$$\begin{aligned}
\text{find} \quad & \lambda(\tau) : [0,1] \to \mathbb{R}^m,\ w(\tau) : [0,1] \to \mathbb{R}^m_+,\ v(\tau) : [0,1] \to \mathbb{R}^m_+, \\
& T \in \mathbb{R},\ x(\tau) : [0,1] \to \mathbb{R}^n && \text{(9a)} \\
\text{s. t.} \quad & TB\lambda(\tau) - TAx(\tau) + x'(\tau) - Te = 0 && \text{(9b)} \\
& (M_{\mathcal{R}} + D)\lambda(\tau) - Cx(\tau) - f + \beta_{\mathcal{R}} = w(\tau) - v(\tau) && \text{(9c)} \\
& \ell_{\mathcal{R}} \leqslant \lambda(\tau) \leqslant u_{\mathcal{R}},\ (\lambda(\tau) - \ell_{\mathcal{R}})^\top w(\tau) = 0,\ (u_{\mathcal{R}} - \lambda(\tau))^\top v(\tau) = 0 && \text{(9d)} \\
& \lambda(0) = \lambda(1),\ x(0) = x(1),\ w(0) = w(1),\ v(0) = v(1), && \text{(9e)}
\end{aligned}$$

where the constraints (9b)–(9d) must hold for any $\tau \in [0, 1]$.

The phase of a periodic solution of an autonomous system is not fixed. Then any time translation of a periodic solution provides another 'different' periodic solution. In other words, if the PWL system admits a periodic solution, it admits an infinite number of periodic solutions each one differing from the others by a translation in time. In order to fix the initial phase of the periodic solution, one more equation is required, which is usually called *anchor equation* [36–38]. A possible anchor equation is the phase condition proposed in [38]:

$$x_j{}'(\hat{\tau}) = Tc_j^\top (Ax(\hat{\tau}) - B\lambda(\hat{\tau}) + e) = 0, \tag{10}$$

where x_j is a generic j-th component of the state at an arbitrarily chosen time instant $\hat{\tau} \in [0, 1]$ and $c_j \in \mathbb{R}^n$ is a vector with all elements equal to zero except for the j-th element equal to 1. Note that the index j can be chosen arbitrarily in the case of sufficiently smooth solutions. Indeed, in the case of periodic solutions $x(t)$ of class C^1, the time derivative of each state variable must be zero at least at one time instant $\hat{\tau} \in [0, 1]$.

In order to solve (9)–(10) with the corresponding constraints, one can discretize (9b) and reformulate the problem in terms of a discrete-time complementarity problem. By using the (θ, γ) discretization technique [39] with a

sampling period $1/N$, N being an integer, and by using the subscript k for indicating the k-th sample of a variable, from (9b) one obtains

$$T\gamma B\lambda_k + T(1-\gamma)B\lambda_{k-1} - T\theta Ax_k - T(1-\theta)Ax_{k-1} + Nx_k - Nx_{k-1} - Te = 0, \tag{11}$$

where $\theta \in [0,1]$ and $\gamma \in [0,1]$. The constraints (9c)–(9d) can be written for each sampling time instant:

$$(M_{\mathcal{R}} + D)\lambda_k - Cx_k - f + \beta_{\mathcal{R}} = w_k - v_k \tag{12a}$$

$$\ell_{\mathcal{R}} \leqslant \lambda_k \leqslant u_{\mathcal{R}}, (\lambda_k - \ell_{\mathcal{R}})^\top w_k = 0, (u_{\mathcal{R}} - \lambda_k)^\top v_k = 0, \tag{12b}$$

with $w_k \geqslant 0$, $v_k \geqslant 0$ and $k = 1, \ldots, N$. Moreover (9e) can be rewritten as

$$\lambda_0 = \lambda_N,\ x_0 = x_N,\ w_0 = w_N,\ v_0 = v_N. \tag{13}$$

Finally, one can assume that $\hat{\tau}$ in (10) is a sampling time instant. Therefore, by defining $\hat{k} = \hat{\tau}N$, the anchor equation (10) can be written as

$$Tc_j^\top (Ax_{\hat{k}} - B\lambda_{\hat{k}} + e) = 0, \tag{14}$$

or, equivalently,

$$x_{\hat{k}} - x_{\hat{k}-1} = 0. \tag{15}$$

By collecting (11)–(13) for $k = 1, \ldots, N$ in a matrix form we are now able to formulate the problem of computing the periodic solution (and its period) as a MQCP. In particular the unknown vector z for the MQCP is given by the samples λ_k and x_k for $k = 1, \ldots, N$ and the period T:

$$z = \mathrm{col}(\overline{\lambda}, \overline{x}, T) = \mathrm{col}(\lambda_1, \ldots, \lambda_N, x_1, \ldots, x_N, T). \tag{16}$$

The lower and upper bounds for T and for each x_k with $k = 1, \ldots, N$ are chosen as $-\infty$ and $+\infty$:

$$\ell = \mathrm{col}(\ell_{\overline{\lambda}}, \ell_{\overline{x}}, l_T) = \mathrm{col}(1_N \otimes \ell_{\mathcal{R}}, -\infty_{N \cdot n}, -\infty) \tag{17a}$$

$$u = \mathrm{col}(u_{\overline{\lambda}}, u_{\overline{x}}, u_T) = \mathrm{col}(1_N \otimes u_{\mathcal{R}}, +\infty_{N \cdot n}, +\infty). \tag{17b}$$

Given the discretization parameters (θ, γ) and the number of discrete samples per period N, by considering (16)–(17), by collecting (11)–(12) for $k = 1, \ldots, N$ together with (13) and by considering (14), the MQCP can be represented in the form (2) with

$$M = \begin{bmatrix} 0 & \overline{G} & \overline{e} \\ \overline{M}_{\mathcal{R}} & \overline{C} & 0 \\ h_\lambda & h_x & 0 \end{bmatrix} \in \mathbb{R}^{(Nn+Nm+1)\times(Nn+Nm+1)} \tag{18a}$$

$$q = \mathrm{col}\,(0_{Nn}, \overline{f}, \delta_q) \in \mathbb{R}^{Nn+Nm+1} \tag{18b}$$

$$\varphi(z) = \mathrm{col}\,(\phi_1(z), \ldots, \phi_N(z), 0_{Nm+1}), \tag{18c}$$

where $\phi_k(z) : \mathbb{R}^{Nn+Nm+1} \to \mathbb{R}^n$ are given by

$$\phi_k(z) = T\gamma B\lambda_k + T(1-\gamma)B\lambda_{k-1} - T\theta Ax_k - T(1-\theta)Ax_{k-1}, \tag{19}$$

for $k = 1, \ldots, N$ together with (13), and

$$\overline{G} = N\Gamma_N(I_n, -I_n) \tag{20a}$$
$$\overline{e} = -1_N \otimes e \tag{20b}$$
$$\overline{M}_{\mathcal{R}} = I_N \otimes (M_{\mathcal{R}} + D) \tag{20c}$$
$$\overline{C} = -I_N \otimes C \tag{20d}$$
$$\overline{f} = 1_N \otimes (-f + \beta_{\mathcal{R}}), \tag{20e}$$

$h_\lambda^\top \in \mathbb{R}^{Nm}$ is a vector with all zero elements, $h_x^\top \in \mathbb{R}^{Nn}$ is a vector with all zero entries but two elements -1 and $+1$ corresponding to the j-th component of $x_{\hat{k}-1}$ and $x_{\hat{k}}$, representing the anchor equation (15), and $\delta_q = 0$. The described formulation is used to compute a stable periodic oscillation in a neural oscillator and an unstable periodic solution in a deadzone feedback system in Sects. 5.1 and 5.2, respectively. Indeed, in such examples the feedback characteristic is Lipschitz continuous, then a solution of class C^1 is expected.

If $x(t)$ is of class C^0, as in the case of a relay feedback system, we have to pay attention to the fact that the time derivative can jump, so a different phase constraint should be derived. In particular, we assume that there exists a component of the system output, say $c_j^\top y$, which is equal to a value α_j at a time instant $\hat{\tau} \in [0, 1]$:

$$c_j^\top y = c_j^\top (Cx(\hat{\tau}) - D\lambda(\hat{\tau}) + f) = \alpha_j. \tag{21}$$

The constant α_j should be selected by exploiting the system structure. In particular, since we use the phase condition (21) because the trajectory $x(t)$ is only C^0, the discontinuity of the time derivative $\dot{x}(t)$ allows to say that there exist some j and $\hat{\tau} \in [0, 1]$ such that (21) holds with α_j being a discontinuity point of the relation $\mathcal{R}_j$.

As in the previous case, we write (21) in discrete-time as follows

$$c_j^\top (Cx_{\hat{k}} - D\lambda_{\hat{k}} + f) = \alpha_j, \tag{22}$$

with $\hat{k} = \hat{\tau}N$. The anchor equation (22) can be included in the form (18) by setting h_λ and h_x with all zero entries except for the components corresponding to $\hat{k}$ which are equal to $-c_j^\top D$ and $c_j^\top C$, respectively, and $\delta_q = c_j^\top f - \alpha_j$. In Sects. 5.3 and 5.4, the anchor equation (22) is used to compute periodic nonsmooth oscillations in a stick-slip system and in a repressilator.

The continuous PWL interpolation of the sequence x_k obtained by solving the MQCP derived above is expected to approximate better and better the continuous-time periodic solution $x(t)$ of (7) as the number of samples per period N increases. Such convergence property of the discrete-time solution is also called 'consistency' [40]. A formal proof of consistency of the solution of time-stepping methods used for solving boundary-value differential variational inequalities can be found in [41]. However, the nonsingularity condition of matrices involved in the boundary-value constraint is not valid in the case of periodic solutions.

4 Equilibrium points and known period

In this section, the MQCP formulated above is specified under two interesting conditions, i.e., when more equilibrium points coexist and when the period of the oscillation is known.

4.1 Elimination of equilibrium points

Depending on the relation $(y, \lambda) \in \mathcal{R}$, constant solutions of (7) are also possible. For instance, when e and f are zero and $(0, 0) \in \mathcal{R}$, the origin is also a solution (an equilibrium) of the system. Since we are interested in nonconstant periodic solutions and the phase constraints (10) and (21) do not exclude the trivial solution (and more in general equilibrium points), one must add a further constraint which excludes the zero solution. To this aim the following condition can be used

$$x_{(\bullet,\hat{\imath})}^{\top} x_{(\bullet,\hat{\imath})} > 0 \tag{23}$$

for some chosen $\hat{\imath}$, where $x_{(\bullet,\hat{\imath})} \in \mathbb{R}^N$ is the vector obtained by collecting all samples of the $\hat{\imath}$-th component of the state vector. The condition (23) can be included in the MQCP by using the following complementarity representation

$$\text{find} \quad z_\rho \in \mathbb{R},\ w_\rho \in \mathbb{R}_+,\ v_\rho \in \mathbb{R}_+ \tag{24a}$$

$$\text{s. t.} \quad x_{(\bullet,\hat{\imath})}^{\top} x_{(\bullet,\hat{\imath})} - \epsilon = w_\rho - v_\rho \tag{24b}$$

$$\ell_\rho \leqslant z_\rho \leqslant u_\rho, (z_\rho - \ell_\rho) w_\rho = 0, (u_\rho - z_\rho) v_\rho = 0, \tag{24c}$$

where ϵ is a small positive parameter, with $\ell_\rho = 0$ and u_ρ equal to $+\infty$ (so that $v_\rho = 0$). Indeed, from the nonnegativity of the variable w_ρ, the constraints (24b) with $v_\rho = 0$ implies that $x_{(\bullet,\hat{\imath})}^{\top} x_{(\bullet,\hat{\imath})}$ must be strictly positive. This approach can be simply extended for the elimination of nonzero equilibrium points.

4.2 MLCP for known period

A particular case of MQCP occurs when the period T of the periodic solution is known. In this case, the periodic solution computation can be formulated in terms of a MLCP. Since T is known, equations (11) are linear with respect to the unknowns λ_k and x_k. By collecting (11) and (12a) for $k = 1, \ldots, N$, by defining ℓ and u as in (17) without the last element and by using the periodicity condition (13), one obtains

$$\overline{B}\,\overline{\lambda} + \overline{A}\overline{x} + \overline{e} = 0 \tag{25a}$$

$$\overline{M}_{\mathcal{R}}\overline{\lambda} + \overline{C}\overline{x} + \overline{f} = \overline{w} - \overline{v}, \tag{25b}$$

with

$$\overline{A} = \Gamma_N \left(I_n - \frac{T}{N}\theta A, -I_n - \frac{T}{N}(1-\theta)A \right) \tag{26a}$$

$$\overline{B} = \frac{T}{N}\Gamma_N \left(\gamma B, (1-\gamma)B \right), \tag{26b}$$

and $\overline{e}$, $\overline{M}_{\mathcal{R}}$, $\overline{C}$ and $\overline{f}$ defined as in (20b)–(20e), respectively.

Since T is known, the anchor equation (10) is not required anymore. In this case, we can define $z = \mathrm{col}(\overline{\lambda}, \overline{x})$ and formulate the above problem as a MLCP, that is (2) without $\varphi(z)$, with the following matrices

$$M = \begin{bmatrix} \overline{M}_{\mathcal{R}} & \overline{C} \\ \overline{B} & \overline{A} \end{bmatrix} \quad \text{and} \quad q = \begin{bmatrix} \overline{f} \\ \overline{e} \end{bmatrix}. \tag{27}$$

In the particular case of a nonsingular $\overline{A}$, one can solve (25a) for the vector $\overline{x}$ thus obtaining

$$\overline{x} = -\overline{A}^{-1}(\overline{B}\,\overline{\lambda} + \overline{e}). \tag{28}$$

By substituting (28) in (25b) one obtains

$$(\overline{M}_{\mathcal{R}} - \overline{CA}^{-1}\overline{B})\overline{\lambda} + \overline{f} - \overline{CA}^{-1}\overline{e} = \overline{w} - \overline{v}, \tag{29}$$

which is in the form (2b) without $\varphi(z)$ and with $z = \overline{\lambda}$, $M = \overline{M}_{\mathcal{R}} - \overline{CA}^{-1}\overline{B}$ and $q = \overline{f} - \overline{CA}^{-1}\overline{e}$. The solution $\overline{\lambda}$ of the corresponding MLCP can be used for the computation of the periodic solution $\overline{x}$ by using (28).

Note that for $T/N \to 0$, the determinant of $\overline{A}$ tends to zero. Then we can state that when a high accuracy is required, i.e., a small step size T/N, the formulation in (25) is preferable to (29).

In the case that the PWL system presents constant solutions, the complementarity problem can be reformulated so that the new problem has no constant solutions. Since the use of (24) makes the problem nonlinear, in order to preserve the linearity we can use an alternative approach.

As an example, let assume that the PWL system has the origin as an equilibrium point, as discussed at the beginning of Sect. 4.1. In order to find only nonzero solutions, one can impose (without loss of generality) x_k to be greater than some positive value ε for some chosen $\bar{k}$. In particular, the constraint $x_{\bar{k}} \geqslant \varepsilon$ can be written in the complementarity form by modifying the constraints on some samples of the vector $\overline{x}$. For instance, one can set $\ell_{x_{\bar{k},1}} = \varepsilon$ and $u_{x_{\bar{k},1}} = +\infty$, where $\ell_{x_{\bar{k},1}}$, $u_{x_{\bar{k},1}}$ are the lower bound and the upper bound of the first component of x at the time $\bar{k}$. Note that the approach presented above is not required in the case of an unknown period, indeed such further constraint affects the phase condition of the solution which is already determined by the anchor equation.

5 Examples

In this section, the effectiveness of the proposed technique for the computation of period and waveform of oscillations is shown by considering PWL systems with different steady-state behaviors. We present a neural oscillator and a deadzone feedback system, which have solutions belonging to class C^1. The second group of examples, including a stick-slip system and a repressilator, present oscillations of class C^0. The computation of the periodic solution and the corresponding period is obtained by solving a MQCP with the matrices given in (18).

For all the following examples, we have computed the 'exact' steady-state solution of the discretized system by constructing the nonlinear *closed-loop* map. The idea for obtaining such map is to consider the solutions of the differential state equations, which model the 'modes' of the system, and to cascade them in order to link a sampled state to the next sample. It is important to highlight that the exact solution can be analytically obtained only if the sequence of modes is known. We numerically show that by varying the number of samples per period, i.e., by improving the resolution of the discretization, the error between the solution obtained with the MQCP and the exact one decreases. The maximum number of samples is chosen for a reasonable computational effort to perform the MATLAB code on a Intel Core i7 clocked at 2.40 GHz. The complementarity problems have been solved by using the PATH solver [32]. The numerical results are also compared by varying the discretization parameters.

5.1 Stable periodic solution in a neural oscillator

The dynamical model of a neural network consisting of η mutually inhibiting neurons with adaptation can be represented in the following form [42]:

$$\tau_1 \dot{\chi}_i = -\chi_i - \kappa v_i - \nu \sum_{j=1, j\neq i}^{\eta} u_j + e_c \tag{30a}$$

$$\tau_2 \dot{v}_i = -v_i + u_i \tag{30b}$$

$$u_i = \max\{0, \chi_i\}, \tag{30c}$$

with $i = 1, \ldots, \eta$. Here, χ_i is the membrane potential of the i-th neuron, v_i represents the degree of adaptation, e_c is the total input from outside the network that is assumed positive and constant with the time, τ_1 is a time constant, τ_2 and κ are the parameters that specify the time course of the adaptation and ν indicates the strength of the inhibitory connection between the neurons. In [42], it is shown that for certain values of the model parameters, the neural network has no stable equilibrium points and produces sustained oscillations. In the following, we consider a neural network with two neurons, i.e., $\eta = 2$. For the neuron 1 and the neuron 2, let us denote by x_1 and x_3 the state variables that represent the membrane potential, respectively, and by x_2

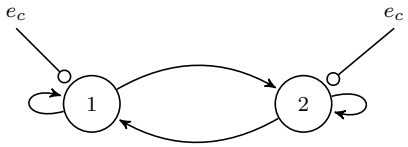

Fig. 3 Neural oscillator scheme.

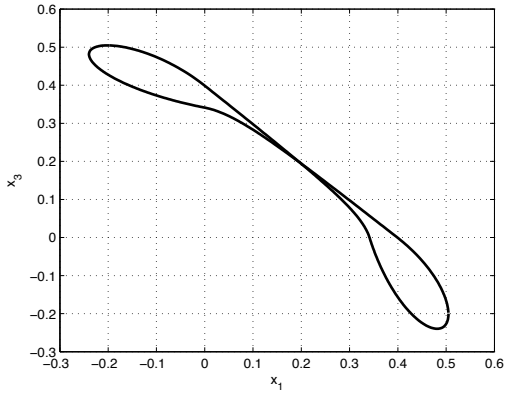

Fig. 4 Stable periodic steady-state oscillation of the neural oscillator projected into the (x_1, x_3) plane.

and x_4 the state variables for the degree of self-inhibition, respectively. Then the neural oscillator can be represented in the form (3) with the following matrices

$$A_u = \begin{bmatrix} -\frac{1}{\tau_1} & -\frac{\kappa}{\tau_1} & 0 & 0 \\ 0 & -\frac{1}{\tau_2} & 0 & 0 \\ 0 & 0 & -\frac{1}{\tau_1} & -\frac{\kappa}{\tau_1} \\ 0 & 0 & 0 & -\frac{1}{\tau_2} \end{bmatrix}, \quad B_u = \begin{bmatrix} 0 & -\frac{\nu}{\tau_1} \\ \frac{1}{\tau_2} & 0 \\ -\frac{\nu}{\tau_1} & 0 \\ 0 & \frac{1}{\tau_2} \end{bmatrix}, \quad e_u = \begin{bmatrix} e_c \\ 0 \\ e_c \\ 0 \end{bmatrix}, \tag{31a}$$

$$C_u = \begin{bmatrix} 1\,0\,0\,0 \\ 0\,0\,1\,0 \end{bmatrix}, \quad D_u = \begin{bmatrix} 0\,0 \\ 0\,0 \end{bmatrix}, \quad f_u = \begin{bmatrix} 0 \\ 0 \end{bmatrix}. \tag{31b}$$

The relation $\mathcal{R} = \mathrm{col}(\mathcal{R}_1, \mathcal{R}_2)$ represents the inhibitory connection between the two neurons, with $\mathcal{R}_i$ that corresponds to $\lambda_i = \max\{0, y_i\}$, $i = 1, 2$, so as indicated by (30c). Each $\mathcal{R}_i$ can be modeled as in (4) with $\mu_i = 1$, $\beta_{\mathcal{R}_i} = 0$, $\ell_i = 0$ and $u_i = +\infty$, and they can be 'linked' to the system by choosing $H_u = -I_2$ and $H_y = I_2$, in (3c) and (3d), respectively. By using (6), the neural model network is recast in form (7a) and (7b) and the feedback relation is represented by the complementarity form discussed above.

In [43], it is shown that by considering the parameters $\tau_1 = 0.1\,\mathrm{s}$, $\tau_2 = 0.2\,\mathrm{s}$, $\kappa = 2$, $\nu = 2$ and $e_c = 1$, the system has a locally stable periodic oscillation. Figure 4 shows the solution computed by solving the corresponding

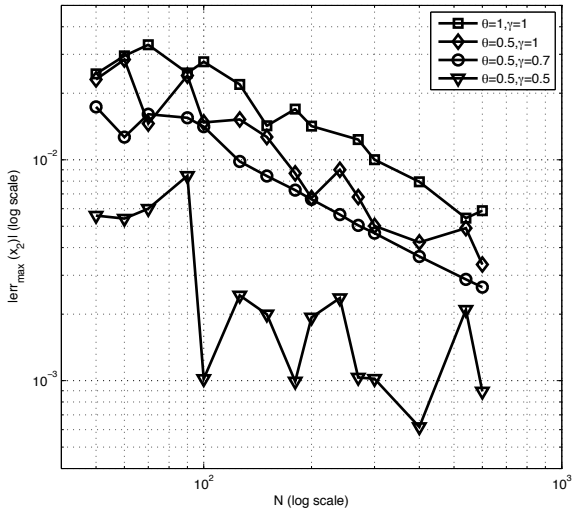

Fig. 5 Neural system. Error in the steady-state solution computation obtained with different discretization techniques and with $N \in [50, 600]$: maximum error in the x_2 trajectory.

MQCP with $N = 600$, $\theta = 0.5$ and $\gamma = 0.5$ that yields a value of the period $T = 0.8973\,\mathrm{s}$. The neural system has also a constant unstable solution in $[0.2, 0.2, 0.2, 0.2]$, that was eliminated by following the procedure presented in Sect. 4.1. Let us consider the error between the exact solution and the solution computed with the complementarity approach by varying the number of samples per period and the parameters θ and γ. Since the relation $\mathcal{R}$ is a Lipschitz continuous function of x, the solution is expected to belong to the class C^1. As suggested in [3], in the case of solutions of class C^1, it is possible to compute the solution of the discretized system by varying both θ and γ in order to obtain the pair which provides the best accuracy for the solution. Figure 5 shows the evolution of the maximum error in the computation of the x_2 trajectory, while in Fig. 6 it is reported the error for the period computation.

As one could expect, the error decreases when the number of samples increases. For $\theta = 0.5$ and γ assuming values between 0.5 and 1, the accuracy is improved, but we do not achieve order 2 when $\gamma = 0.5$. This in mainly due to the lack of regularity of the computed solution. This phenomenon is generally observed when higher order methods are used for a solution with limited smoothness, see [4, §9.1].

5.2 Unstable periodic solution in a deadzone feedback system

The deadzone behaviour is typical in many real actuator systems, including mechanical connections, hydraulic servo valves, piezoelectric translators, and

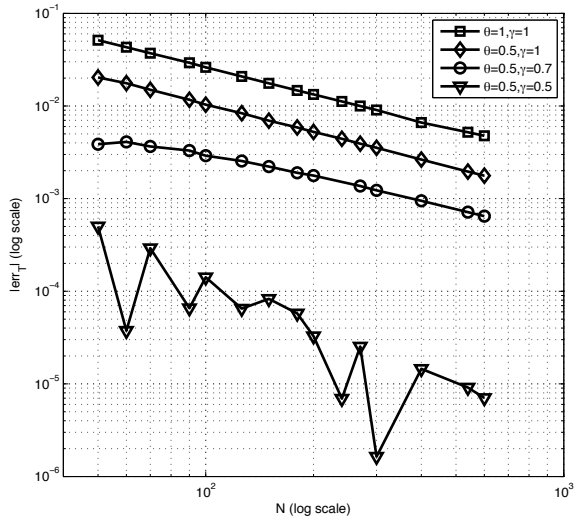

Fig. 6 Neural system. Error in the period computation obtained with different discretization techniques and with $N \in [50, 600]$.

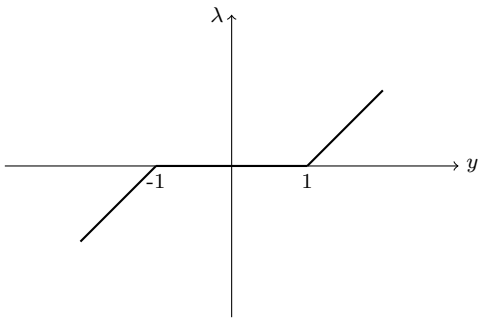

Fig. 7 Deadzone characteristic.

electronic circuits. A graphical representation is given in Fig. 7 and an analytical description is presented below

$$\lambda = \begin{cases} y-1 & \text{if } y > 1 \\ 0 & \text{if } -1 \leqslant y \leqslant 1 \\ y+1 & \text{if } y < -1 \end{cases} . \tag{32}$$

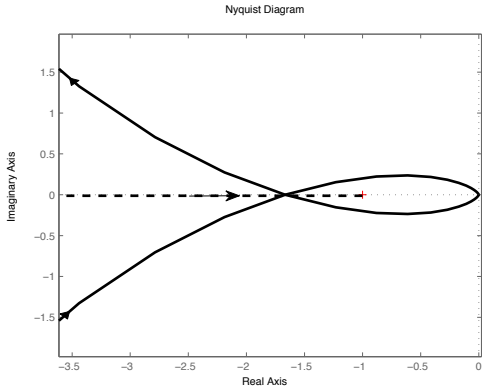

Fig. 8 Nyquist diagram of the transfer function of the dynamical system (continuous line) together with the representation of the negative reciprocal of the deadzone describing function (dashed line).

In this section, we analyze the steady-state periodic behaviour of the dynamical system in form (3) with the following matrices

$$A_u = \begin{bmatrix} 0 & 1 & 0 \\ 0 & 0 & 1 \\ 0 & -3 & -4 \end{bmatrix}, \qquad B_u = \begin{bmatrix} 0 \\ 0 \\ 20 \end{bmatrix}, \qquad e_u = \begin{bmatrix} 0 \\ 0 \\ 0 \end{bmatrix}, \tag{33a}$$

$$C_u = \begin{bmatrix} 1 & 0 & 0 \end{bmatrix}, \qquad D_u = 0, \qquad f_u = 0, \tag{33b}$$

and whose feedback characteristic is the deadzone in Fig. 7. Note that A is not Hurwitz, then self-induced oscillation are possible [44].

The dynamical system is a low-pass filter and the polar diagram intersects the negative real axis, so the closed-loop system is a good candidate for the application of the describing function technique [45]. The value of the approximated period is computed by considering the oscillation frequency ω^* corresponding to the point in which the polar diagram of $G(j\omega)$ (continuous line in Fig. 8) intersects the negative reciprocal of the describing function graph (dashed line in Fig. 8). We obtain $\omega^* = 1.723$ rad/s, then the corresponding period $T^* = 3.627$ s. Moreover, the orientation of the two curves predicts that the periodic oscillation is unstable.

The following numerical results show that the proposed complementarity approach is able to get the periodic behaviour together with the period also in the case of unstable solutions. The deadzone characteristic can be expressed as the difference of two saturation-like characteristics, $\mathcal{R}_1$ and $\mathcal{R}_2$. In particular, $\mathcal{R}_1$ corresponds to $\lambda_1 = y_1$, while $\mathcal{R}_2$ is $\lambda_2 = \mathrm{sat}(y_2)$, that is the unitary saturation function. These two relations can be modelled as in (4) by choosing for $\mathcal{R}_1$, $\mu_1 = 0$, $\beta_{\mathcal{R}_1} = 0$, $\ell_1 = -\infty$ and $u_1 = +\infty$, while for $\mathcal{R}_2$, $\mu_2 = 1$, $\beta_{\mathcal{R}_2} = 0$, $\ell_2 = -1$ and $u_2 = +1$. Then we choose $H_u = \begin{bmatrix} 1, -1 \end{bmatrix}$ and $H_y = \mathrm{col}(1, 1)$ in (3c) and (3d), respectively. By using (6), the dynamical system can be recast

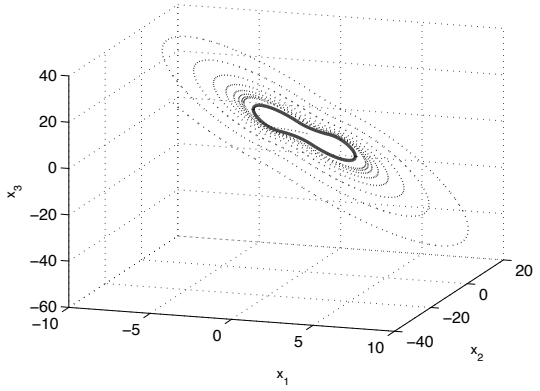

Fig. 9 Unstable periodic oscillation for the deadzone feedback system: steady-state solution computed by using the MQCP approach (continuous line) and diverging time-stepping simulation (dotted line).

in form (7a) and (7b), together with the complementarity representation of feedback relation discussed above.

Figure 9 shows the periodic solution computed through the proposed technique, by solving a MQCP with matrices in (18) and, with $N = 5400$, $\theta = 0.5$ and $\gamma = 0.5$, which yields to a value of the period $T = 3.6620\,\mathrm{s}$. The dotted line graph corresponds to the numerical result obtained by implementing a time-stepping simulation of the initial value problem [3,46], with an initial condition sufficiently close to the periodic solution ($x_0 = \big[1.3, -7.848, 4\big]$).

The error between the exact solution and the one computed with the complementarity approach has been analyzed by varying the number of samples per period between 100 and 5400 and by considering values of the parameters θ and γ in the interval $[0.5, 1]$, see Fig. 10 and Fig. 11. It is possible to prove that the trivial solution is also a solution of the system considered in this example, so the constraint (24) was added to the problem (18) to directly get the periodic solution.

Qualitatively, the same comments presented for the previous example about the accuracy of the error can be repeated, see Figs. 5 and 6.

5.3 Sliding periodic solution in a stick-slip system

Let us consider a mass m connected to a spring with elastic constant K, which is pulled at a constant speed e_s. Let x_1 be the elongation of the spring, and x_2 the mass velocity. Such system can be represented in the form (3) with

$$A_u = \begin{bmatrix} 0 & -1 \\ \frac{K}{m} & 0 \end{bmatrix}, \qquad B_u = \begin{bmatrix} 0 \\ \frac{1}{m} \end{bmatrix}, \qquad e_u = \begin{bmatrix} e_s \\ 0 \end{bmatrix}, \tag{34a}$$

$$C_u = \begin{bmatrix} 0 & 1 \end{bmatrix}, \qquad D_u = 0, \qquad f_u = 0, \tag{34b}$$

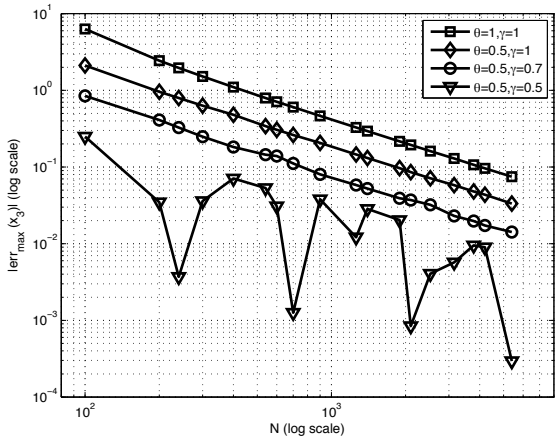

Fig. 10 Deadzone feedback system. Error in the steady-state solution computation obtained with different discretization techniques and with $N \in [100, 5400]$: maximum error in the x_3 trajectory.

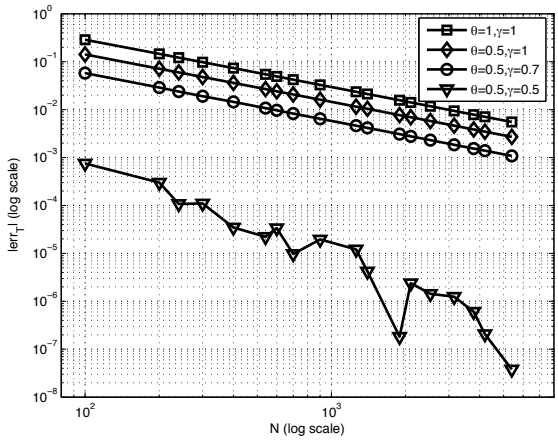

Fig. 11 Deadzone feedback system. Error in the period computation obtained with different discretization techniques and with $N \in [100, 5400]$.

and $\mathcal{R}$ being the friction characteristic represented in Fig. 12, where F_c and F_s are the Coulomb friction and the stiction force, respectively. As in the previous example, such characteristic can be obtained as the combination of two saturation-like characteristics, say $\mathcal{R}_1$ and $\mathcal{R}_2$. In this case, $\mathcal{R}_1$ represents $\lambda_1 = \text{relay}(y_1)$, where $\text{relay}(\cdot)$ is the unitary relay characteristic, and $\mathcal{R}_2$ is $\lambda_2 = \text{sat}_{m_\mathcal{R}}(y_2)$, where $\text{sat}_{m_\mathcal{R}}(\cdot)$ is the unitary saturation function where the nonzero slope of the characteristic is $1/m_\mathcal{R}$. The two relations can be modelled as in (4) by choosing for $\mathcal{R}_1$, $\mu_1 = 0$, $\beta_{\mathcal{R}_1} = 0$, $\ell_1 = -1$ and $u_1 = +1$,

and for $\mathcal{R}_2$, $\mu_2 = m_{\mathcal{R}}$, $\beta_{\mathcal{R}_2} = 0$, $\ell_2 = -1$ and $u_2 = +1$. Then we choose $H_u = \left[F_s, -(F_s - F_c)\right]$ and $H_y = \mathrm{col}(1, 1)$ in (3c) and (3d), respectively, and we write the dynamical system in form (7) with the matrices given by (6).

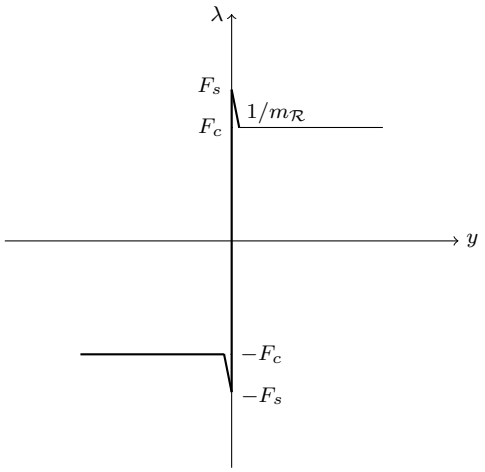

Fig. 12 Coulomb friction characteristic with Stribeck effect with null viscous friction: y is the mass velocity and λ is the friction force.

Let us select $m = 1$ kg, $K = 2\,\mathrm{N/m}$, $F_c = 2.94\,\mathrm{N}$, $F_s = 5.88\,\mathrm{N}$, $m_{\mathcal{R}} = 1/12$, and $e_s = 2\,\mathrm{m/s}$. In [47], it is shown that this system can exhibit complex behaviors and that, depending on the selection of the integration technique, it is possible that sticking phases of the mass can be missed by the numerical simulation. Due to the discontinuity of the PWL relation at $y = 0$, a solution belonging to C^0 is expected. For such reason, the computation of the periodic solution and the corresponding period was obtained by solving the MQCP with matrices given in (18), replacing the anchor equation with the one in (22). Figure 13 shows that the complementarity approach is able to get the steady-state periodic behaviour of the system, in which it is possible to recognize the stick and the slip mode. When the trajectory is in the stick mode the friction force increases rapidly and stops the motion. The system remains in the stick mode as long as the spring force is smaller than the stiction force. After that, the system enters in the slip mode and the mass accelerates subject to the Coulomb friction. The spring is then compressed and the motion of the mass stops again and the spring force needs to win again the stiction force. Such solution is computed by solving the complementarity problem (12) with $N = 1000$, $\theta = 0.5$ and $\gamma = 1$ that yields a period $T = 4.9355\,\mathrm{s}$ and by eliminating the equilibrium point in $[F_c/K, e_s]$ by following the procedure in Sect. 4.1. Since the smoothness of the solution is one degree lower with respect to the previous examples, according to the discretization scheme in [4], we have fixed $\gamma = 1$ and we have varied only θ. The evolution of the error shown in Figs. 14 and 15 confirms the effectiveness of the proposed approach.

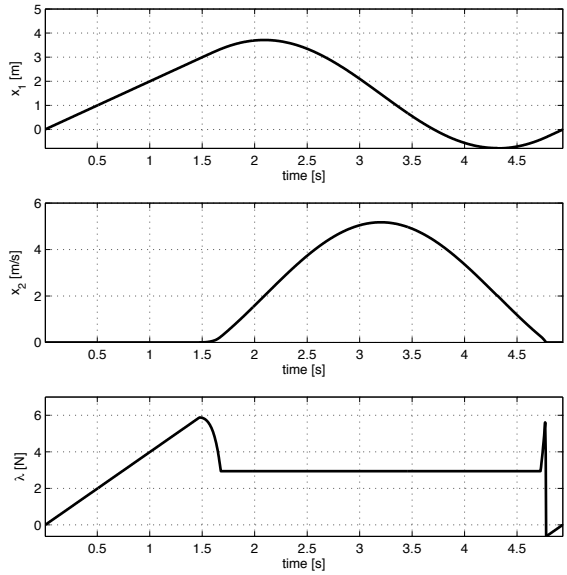

Fig. 13 Periodic steady-state solution of the stick-slip system. The graphs show the elongation of the spring, x_1, the velocity of the mass, x_2 and the friction force, λ. The solution is obtained by fixing $N = 1000$, $\theta = 0.5$ and $\gamma = 1$. The corresponding value of the period is 4.9355 s.

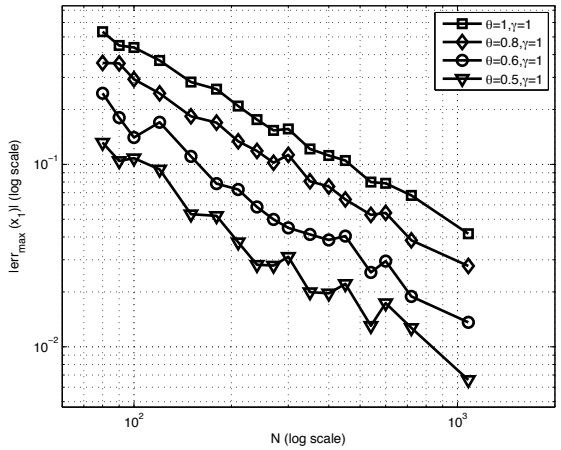

Fig. 14 Stick-slip system. Error in the steady-state solution computed with different discretization techniques and with $N \in [90, 1080]$: maximum error in the x_1 trajectory.

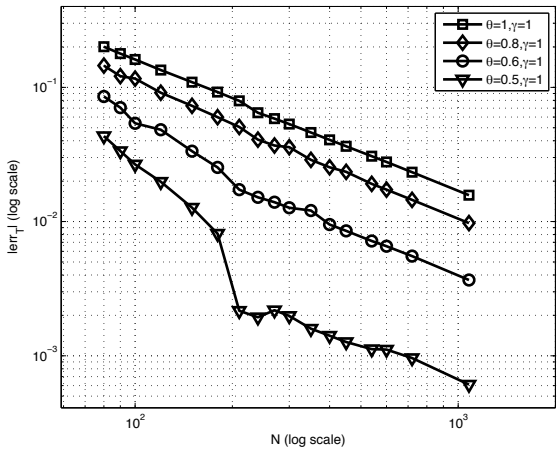

Fig. 15 Stick-slip system. Error in the steady-state period computation obtained with different discretization techniques and with $N \in [90, 1080]$.

5.4 Nonsmooth stable periodic solution in a repressilator

Let us now consider the model of a repressilator, which is a synthetic genetic regulatory network that uses a cyclic repression structure. In the literature (see, e.g., [48] and the reference therein) it is shown the existence of oscillations for a three dimensional system in which the sigmoidal regulation functions that determine the interaction between the elements of the network is replaced by step functions. The resulting PWL systems have been proposed as a modelling framework in biology allowing efficient simulations, as confirmed in [49] where the complementarity approach is used to compute the behavior of a repressilator in the bacterium *Escherichia coli*. Such a repressilator consists of three genes and it can be modelled by considering the evolution of three variables which represent the concentrations of the proteins LacI, TetR, and CI. Such a repressilator model can be easily put in the form (3) with

$$A_u = \begin{bmatrix} -a_1 & 0 & 0 \\ 0 & -a_2 & 0 \\ 0 & 0 & -a_3 \end{bmatrix}, \qquad B_u = \begin{bmatrix} -b_1 & 0 & 0 \\ 0 & -b_2 & 0 \\ 0 & 0 & -b_3 \end{bmatrix}, \qquad e_u = \begin{bmatrix} e_1 \\ e_2 \\ e_3 \end{bmatrix}, \tag{35a}$$

$$C_u = \begin{bmatrix} 0\,0\,1 \\ 1\,0\,0 \\ 0\,1\,0 \end{bmatrix}, \qquad D_u = 0, \qquad f_u = 0, \tag{35b}$$

and $\mathcal{R} = \mathrm{col}\{\mathcal{R}_1, \mathcal{R}_2, \mathcal{R}_3\}$ where

$$\lambda_i = \begin{cases} 0 & \text{if } y_i > 1 \\ [0,1] & \text{if } y_i = 1 \\ 1 & \text{if } y_i < 1 \end{cases}, \tag{36}$$

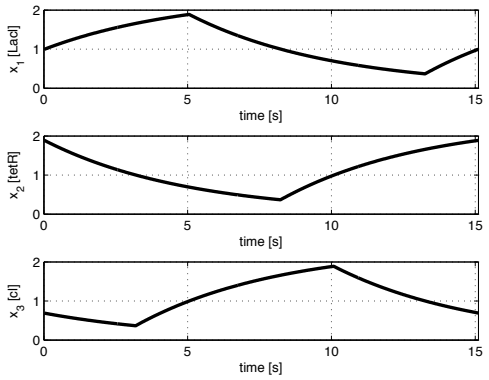

Fig. 16 Periodic steady-state solution of a repressilator network consisting of three genes. The graph shows the evolution of the variables x_1, x_2 and x_3 which represent the concentration of proteins LacI, Tetr and Cl, respectively. The solution is obtained by fixing N=1080, $\theta = 0.5$ and $\gamma = 1$. The corresponding value of the period is $T = 15.1116$ s.

and $i = 1, 2, 3$. Each relation $\mathcal{R}_i$ can be modelled as the MLCP (4) with $\mu_i = 0$, $\beta_{\mathcal{R}_i} = -1$, $\ell_i = 0$ and $u_i = 1$. Then we choose $H_u = I_3$ and $H_y = -I_3$ in (3c) and (3d), respectively, and we write the dynamical system in form (7) with the matrices given by (6).

As showed in [49], the system has an unstable equilibrium point in $(1, 1, 1)$ and a stable nonsmooth periodic solution. In order to compute such solution and the associated period, we solve a MQCP with matrices in (18) replacing the anchor equation with the one in (22).

Figure 16 shows the time evolution of the periodic steady-state for the state variables, obtained with the proposed approach. The error results in Fig. 17 show that for this particular example the solution is not much sensitive to the discretization parameters.

6 Conclusions

The mixed quadratic complementarity approach has been proposed for the computation of periodic solutions in a class of piecewise linear (PWL) systems, which consist of linear time-invariant systems with PWL feedback relations representable as linear combinations of saturation-like or step characteristics. For many practical systems belonging to this class the period and the shape of the oscillation is difficult to be predicted, then phase conditions acting as anchor equations for the periodic solution have been added to the complementarity problem. It has been shown how the discretization of the closed-loop system together with the periodicity constraint and the phase condition permits to build a mixed quadratic complementarity problem whose solution corresponds to the searched periodic solution and to the corresponding period. The effec-

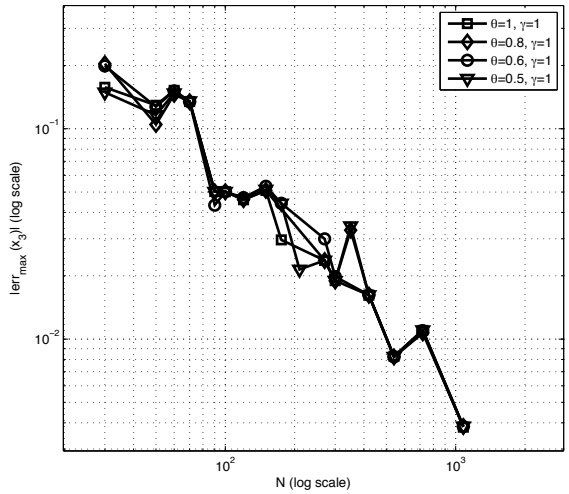

Fig. 17 Repressilator network. Error in the steady-state solution computation obtained with different discretization techniques and with $N \in [30, 1080]$: maximum error in the x_3 trajectory.

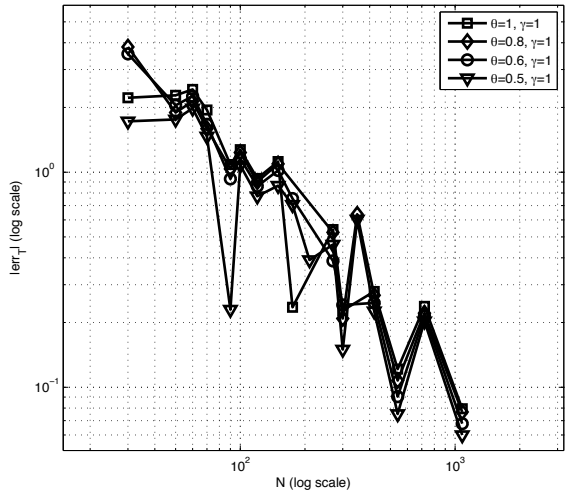

Fig. 18 Repressilator network. Error in the steady-state period computation obtained with different discretization techniques and with $N \in [30, 1080]$.

tiveness of the proposed approach has been tested by considering several practical PWL systems with different steady-state periodic behaviours: a stable periodic solution in a neural oscillator, an unstable oscillation for a deadzone feedback system, a sliding orbit in a stick-slip system and a periodic solution beloging to a repressilator. The simulations, implemented by using different discretization schemes and sampling frequencies, show the good accuracy of the proposed approach with respect to the analytical solution, computed by assuming the a priori knowledge of the modes sequence.

References

1. T. E. Stern. Piecewise-linear network theory. Technical report, PhD thesis, MIT, Research Laboratory of Electronics, Cambridge, MA, USA, 1956.
2. M. K. Camlibel, W. P. M. H. Heemels, A. J. van der Schaft, and J. M. Schumacher. Switched networks and complementarity. *IEEE Trans. Circuits Syst. I, Reg. Papers*, 50(8):1036–1046, 2003.
3. V. Acary, O. Bonnefon, and B. Brogliato. Time-stepping numerical simulation of switched circuits within the nonsmooth dynamical systems approach. *IEEE Trans. Comput.-Aided Design Integr. Circuits Syst.*, 29(7):1042–1055, 2010.
4. V. Acary and B. Brogliato. *Numerical methods for nonsmooth dynamical systems.* Berlin Heidelberg: Springer-Verlag, 2008.
5. J. Melin, A. Hultgren, and T. Lindstrom. Two types of limit cycles of a resonant converter modelled by three-dimensional system. *Nonlinear Analysis: Hybrid Systems*, 2(4):1275–1286, 2008.
6. X-S. Yang and G. Chen. Limit cycle and chaotic invariant sets in autonomous hybrid planar systems. *Nonlinear Analysis: Hybrid Systems*, 2(3):952–957, 2008.
7. T. Aprille and T. Trick. A computer algorithm to determine the steady-state response of nonlinear oscillators. *IEEE Trans. Circuit Theory*, 19(4):354–360, 1972.
8. D. Flieller, P. Riedinger, and J. P. Louis. Computation and stability of limit cycles in hybrid systems. *Nonlinear Analysis: Theory, Methods & Applications*, 64(2):352–367, 2006.
9. D. Li and J. Xu. A new method to determine the periodic orbit of a nonlinear dynamic systems and its period. *Engineering with Computers*, 20(4):316–322, 2005.
10. R. I. Leine and H. Nijmeijer. *Dynamics and Bifurcations of Non-Smooth Mechanical Systems.* London, UK: Springer Verlag, 2004.
11. C. Theodosiou, A. Pournaras, and S. Natsiavas. On periodic steady state response and stability of Filippov-type mechanical models. *Nonlinear Dyn.*, 66(3):355–376, 2011.
12. F. Bizzarri, A. Brambilla, and G. Storti Gajani. Steady state computation and noise analysis of analog mixed signal circuits. *IEEE Trans. Circuits Syst. I, Reg. Papers*, 59(3):541–554, 2012.
13. R. I. Leine, D. H. Van Campen, and A. De Kraker. Stick-slip vibrations induced by alternate friction models. *Nonlinear Dyn.*, 16(1):41–54, 1998.
14. B. L. Van De Vrande, D. H. Van Campen, and A. De Kraker. An approximate analysis of dry-friction-induced stick-slip vibrations by smoothing procedure. *Nonlinear Dyn.*, 19(2):157–169, 1999.
15. F. Bonani and M. Gilli. Analysis of stability and bifurcations of limit cycle in Chua's circuit through the Harmonic-Balance approach. *IEEE Trans. Circuits Syst. I, Reg. Papers*, 46(8):881–890, 1999.
16. F. B. Duarte and J. Tenreiro Machado. Fractional describing function of systems with Coulomb friction. *Nonlinear Dyn.*, 56(4):381–387, 2009.
17. Y.-J. Huang and Y.-J. Wang. Steady-state analysis for a class of sliding mode controlled systems using describing function method. *Nonlinear Dyn.*, 30(3):223–241, 2002.
18. S. Engelberg. Limitations of the describing function for limit cycle prediction. *IEEE Trans. Autom. Control*, 47(11):1887–1890, 2002.

19. Chung-Jen Lu and Yu-Min Lin. A modified incremental harmonic balance method for rotary periodic motions. *Nonlinear Dyn.*, 66(4):781–788, 2011.
20. M. Bonnin, M. Gilli, and P. P. Civalleri. A mixed time-frequency-domain approach for the analysis of a hysteretic oscillator. *IEEE Trans. Circuits Syst. II, Exp. Briefs*, 52(9):525–529, 2005.
21. A. Brambilla, G. Gruosso, and G. Storti Gajani. MTFS mixed time-frequency method for the steady-state analysis of almost-periodic nonlinear circuits. *IEEE Trans. Comput.-Aided Design Integr. Circuits Syst.*, 31(9):1346–1355, 2012.
22. F. Vasca, L. Iannelli, and M. K. Camlibel. A new perspective for modeling power electronics converters: complementarity framework. *IEEE Trans. Power Electron.*, 24(2):456–468, 2009.
23. J. M. Schumacher. Complementarity systems in optimization. *Mathematical Programming*, 101(1):4263–296, 2004.
24. V. Sessa, L. Iannelli, and F. Vasca. A complementarity model for closed-loop power converters. IEEE Trans. Power Electron., 2014.
25. A.J. van der Schaft and J.M. Schumacher. Complementarity modeling of hybrid systems. *IEEE Trans. Autom. Control*, 43:483–490, 1998.
26. W. P. M. H Heemels, B. De Schutter, and A. Bemporad. Equivalence of hybrid dynamical model. *Automatica*, 37(7):1085–1091, 2001.
27. L. Iannelli and F. Vasca. Computation of limit cycles and forced oscillations in discrete-time piecewise linear feedback systems through a complementarity approach. In *47th IEEE Conference on Decision and Control*, pages 1169–1174, Cancun, Mexico, Dec. 2008.
28. L. Iannelli, F. Vasca, and V. Sessa. Computation of limit cycles in Lur'e systems. In *American Control Conference*, pages 1402–1407, San Francisco, CA, USA, June 2011.
29. V. Sessa, L. Iannelli, and F. Vasca. Mixed linear complementarity problems for the analysis of limit cycles in piecewise linear systems. In *the 51st IEEE Conference on Decision and Control*, pages 1023 – 1028, Maui, Hawaii, USA, Dec. 2012.
30. V. Sessa, L. Iannelli, V. Acary, B. Brogliato, and F. Vasca. Computing period and shape of oscillations in piecewise linear Lur'e systems: a complementarity approach. In *the 52nd IEEE Conference on Decision and Control*, pages 4680–4685, Florence, Italy, Dec. 2013.
31. F. Facchinei and J. S. Pang. *Finite-Dimensional Variational Inequalities and Complementarity Problems*. Operations Research. Springer-Verlag, New York, 2003.
32. S. P. Dirkse and M. C. Ferris. The PATH solver: a non-monotone stabilization scheme for mixed complementarity problems. *Optimization Methods and Software*, 5:123–156, 1995.
33. R. Cottle, J. Pang, and R. Stone. *The linear complementarity problem*. Academic Press, second edition, 2009.
34. M. S. Gowda and J. Pang. Stability analysis of variational inequalities and nonlinear complementarity problems, via the mixed linear complementarity problem and degree theory. *Mathematics of Operations Research*, 19(4):831–879, 1994.
35. M. Farkas. *Periodic Motions*. Springer-Verlag, New York, Springer Series in Applied mathematical sciences edition, 1994.
36. E. J. Doedel. AUTO: A program for the automatic bifurcation analysis of autonomous systems. *Congressus Numeratium*, 30:1265–1284, 1981.
37. A. H. Nayfeh and B. Balachandran. *Applied Nonlinear Dynamics; Analytical, Computational and Experimental Methods*. Wiley-International, Chichester, 1995.
38. R. U. Seydel. *Practical Bifurcation and Stability Analysis*. Interdisciplinary Applied Mathematics. New York: Springer, third edition, 1988.
39. V. Acary. Time-stepping via complementarity. In F. Vasca and L. Iannelli, editors, *Dynamics and Control of Switched Electroinic Systems*, Advances in Industrial Control. London, U.K.: Springer-Verlag, 2012.
40. L. Han, A. Tiwari, M. K. Camlibel, and J.-S. Pang. Convergence of time-stepping for passive and extended linear complementarity systems. *SIAM J. Numer. Anal.*, 47(5):3768–3796, 2009.
41. J.-S. Pang and D. E. Stewart. Differential variational inequalities. *Math. Program.*, 113:345–424, 2008.

42. K. Matsuoka. Sustained oscillations generated by mutually inhibiting neurons with adaptation. *Biol. Cybern.*, 52:367376, 1985.
43. J. M. Goncalves. Region of stability for limit cycles in piecewise linear systems. *IEEE Trans. Autom. Contr*, 50(11):1877–1882, 2005.
44. T. Hu, T. Thibodeau, and T. R. Teel. A unified Lyapunov approach to analysis of oscillations and stability for systems with piecewise linear elements. *IEEE Trans. Autom. Control*, 55(12):2864–2869, 2010.
45. H. K. Khalil. *Nonlinear systems*. Prentice Hall, New Jersey, 2002.
46. W. P. M. H. Heemels, M. K. Camlibel, and J. M. Schumacher. A time-stepping method for relay systems. In *39th IEEE Conference on Decision and Control*, pages 4461–4466, Sydney, Australia, Dec. 2000.
47. K. J. Astrom and C. Canudas De Wit. Revisiting the LuGre friction model. *IEEE Control Syst. Mag.*, 28(6):101–114, 2008.
48. A. Tonnelier. Cyclic negative feedback systems: what is the chance of oscillation? *Bulletin of Mathematical Biology*, 76(5):1155–1193, 2014.
49. V. Acary, H. de Jong, and B. Brogliato. Numerical simulation of piecewise-linear models of gene regulatory networks using complementarity systems. *Physica D: Nonlinear Phenomena*, 269:103–119, 2014.